☙

# Critical State of the Anderson Transition: Between a Metal and an Insulator

Gabriel Lemarié,[1,*] Hans Lignier,[2,†] Dominique Delande,[1] Pascal Szriftgiser,[2] and Jean Claude Garreau[2]

[1]*Laboratoire Kastler Brossel, UPMC-Paris 6, ENS, CNRS; 4 Place Jussieu, F-75005 Paris, France*
[2]*Laboratoire de Physique des Lasers, Atomes et Molécules, Université Lille 1 Sciences et Technologies, UMR CNRS 8523;
F-59655 Villeneuve d'Ascq Cedex, France[‡]*

Using a three-frequency one-dimensional kicked rotor experimentally realized with a cold atomic gas, we study the transport properties at the critical point of the metal-insulator Anderson transition. We accurately measure the time evolution of an initially localized wave packet and show that it displays at the critical point a scaling invariance characteristic of this second-order phase transition. The shape of the momentum distribution at the critical point is found to be in excellent agreement with the analytical form deduced from the self-consistent theory of localization.

Different phase transitions observed in various fields of physics often share similar characteristics [1]. Of special interest is the behavior of the system at the critical point (for example, scale invariance) and in its immediate vicinity (e.g., divergence of a characteristic length scale). The advent of cold atom physics has offered new possibilities of direct experimental observation of such characteristics of quantum phase transitions. In this Letter, we show that the Anderson metal-insulator transition (recently observed with atomic matter waves [2]) obeys scale invariance at the threshold, defining a new state of matter between a metal and an insulator.

The Anderson transition takes place in three-dimensional (3D) disordered noninteracting systems in the mesoscopic regime (where the transport is coherent). It involves a metallic phase at low disorder associated with an essentially diffusive transport, and an insulating phase at large disorder where transport over long distance is inhibited by interference effects: This is the so-called Anderson localization phenomenon [3]. The Anderson transition is a second-order (continuous) phase transition: On the insulating side, the localization characteristic length $\ell$ diverges algebraically, $\ell \propto |K - K_c|^{-\nu}$ when $K$, the control parameter, approaches the threshold $K_c$ of the transition. On the metallic side, similarly, the diffusion constant vanishes algebraically $D \propto |K - K_c|^s$. The critical exponents $s$ and $\nu$ are equal in 3D, and universal (they do not depend on the microscopic details of the system) [4]. Only recently have these theoretical predictions been confirmed experimentally and the value of $\nu = s$ unambiguously determined [2,5,6]: $\nu = 1.4 \pm 0.3$ is found perfectly compatible with $\nu = 1.57 \pm 0.02$ obtained from numerical simulations of the 3D Anderson model [7].

The state of a disordered system is, in this context, characterized by its transport properties. One can consider the behavior at large distances and long times of the (disorder) averaged intensity Green function (AIGF) which determines the probability $P(\boldsymbol{r}, \boldsymbol{r}'; t)$ for a particle to go from $\boldsymbol{r}$ to $\boldsymbol{r}'$ in time $t$ [8]. In the insulating phase, the AIGF

is a stationary function exponentially localized:

$$P(\boldsymbol{r}, \boldsymbol{r}'; t) \sim \exp(-|\boldsymbol{r} - \boldsymbol{r}'|/2\ell) \qquad \text{[localized]}, \qquad (1)$$

while in the metallic regime, it is a Gaussian expanding diffusively:

$$P(\boldsymbol{r}, \boldsymbol{r}'; t) \sim \exp[-(\boldsymbol{r} - \boldsymbol{r}')^2/2Dt] \qquad \text{[diffusive]}. \qquad (2)$$

These two behaviors are, however, long time asymptotics. Indeed, a localized AIGF is observed only for times $t \gg t_\ell$, where $t_\ell$ is the localization time (the time scale associated to localization). At the transition, $t_\ell \sim \ell^3$ diverges, implying that there is no characteristic time scale; in other words, the system presents a temporal scale invariance. This also implies that the AIGF at the critical point obeys a spatio-temporal scaling law, which is (see below):

$$P(r, r'; t) \sim \exp[-\alpha|\boldsymbol{r} - \boldsymbol{r}'|^{3/2}/t^{1/2}] \qquad \text{[critical]}, \qquad (3)$$

where $\alpha$ is a known (measurable) quantity. This defines a new state, since the shape does not change with time. Such a state of matter, intermediate between an insulator and a metal at any time, has never been directly observed experimentally, although interesting results have recently been published for ultrasound waves in the localized regime [9]. The purpose of this Letter is to report the first experimental characterization of such a critical state of the Anderson transition.

In cold atomic gases, it is possible to prepare the system in a localized state and follow its evolution over time; this constitutes an experimental measurement of the (A)IGF [2,10,11], which is impossible to achieve in state of the art solid state physics. Observing the 3D Anderson transition in configuration space with cold atoms requires a disordered potential with a correlation length comparable to the de Broglie wavelength [12] which has not yet been achieved. Using a spatially quasiperiodic—i.e., nonrandom—potential, a metal-insulator transition (slightly different from the Anderson transition) has been predicted and experimentally observed [13].

We have recently shown [2,5] that it is nevertheless possible to observe Anderson localization and the Anderson transition in momentum space by using a different system, the atomic kicked rotor (described below), where the chaotic nature of the classical motion replaces the disordered potential.

Our atom-optics system (see [5] for a detailed description) consists in a cloud of laser-cooled cesium atoms (FWHM of the momentum distribution of $8\hbar k_L$) interacting with a pulsed (period $T_1 = 27.778$ $\mu$s), far detuned ($\Delta = -11.3$ GHz) standing wave (wave number $k_L = 7.4 \times 10^6$ m$^{-1}$ and one way intensity $I_0 = 150$ mW). The amplitude of the kicks is modulated with two frequencies $\omega_2$ and $\omega_3$. The corresponding Hamiltonian reads

$$H = \frac{p^2}{2} + K \cos x [1 + \varepsilon \cos(\omega_2 t) \cos(\omega_3 t)] \sum_{n=0}^{N-1} \delta(t - n),$$

(4)

where time is measured in units of $T_1$, space in units of $(2k_L)^{-1}$, momentum in units of $2\hbar k_L/\hbar$, with $\hbar = 4\hbar k_L^2 T_1/M = 2.89$ ($M$ is the atom mass) playing the role of an effective Planck constant ($[x, p] = i\hbar$), and $K$ is the average kick amplitude. The kicks are short enough (duration $\tau = 0.8$ $\mu$s) as compared to the atom dynamics so that they can be considered as Dirac delta functions. Decoherence processes, analyzed in detail in [5], are small for the typical duration of the experiment $t \simeq 160$ kicks.

If $\omega_2$, $\omega_3$, $\pi$ and $\hbar$ are incommensurate, this 1D quasiperiodic kicked rotor has been shown to be equivalent to a 3D disordered anisotropic system [6,14,15] and to display

an Anderson metal-insulator transition, as evidenced by the fact that it belongs to the universality class of the orthogonal (characteristic of spinless time-reversal invariant systems) 3D Anderson model [6,7], i.e., has the same critical exponent $\nu$. A peculiarity of the quasiperiodic kicked rotor is that the various quasieigenstates of the system all have the same localization properties, making the experimental measurement of the AIGF easier.

Another peculiarity is that the localization manifests itself in *momentum space* instead of configuration space. We thus expect the AIGF to take simpler forms in momentum space, with expressions similar to Eqs. (1)–(3) (simply replacing position $r$ by momentum $p$). In order to avoid confusion, we will use the notation $\Pi(p, p'; t)$ for the AIGF in momentum space. Thus, an initial momentum distribution $W(p, t = 0)$ will on average evolve at time $t$ to

$$W(p, t) = \int \Pi(p, p'; t) W(p', 0) dp'.$$

(5)

Experimentally, we are able to measure the momentum distribution at the end of a pulse sequence (up to 160 kicks), using Raman stimulated transitions (see [16,17] for details). The initial state $W(p, t = 0)$ is a thermal momentum distribution whose width is much smaller than the width of the final distribution, and can thus be approximated by a $\delta$-function $\delta(p)$ in Eq. (5). As a consequence, the final momentum distribution $W(p, t)$ faithfully measures the intensity Green function $\Pi(p, t) \equiv \Pi(p, 0; t)$.

Figure 1 shows the experimentally measured AIGF $\Pi(p, t)$ at various times in the localized, critical, and
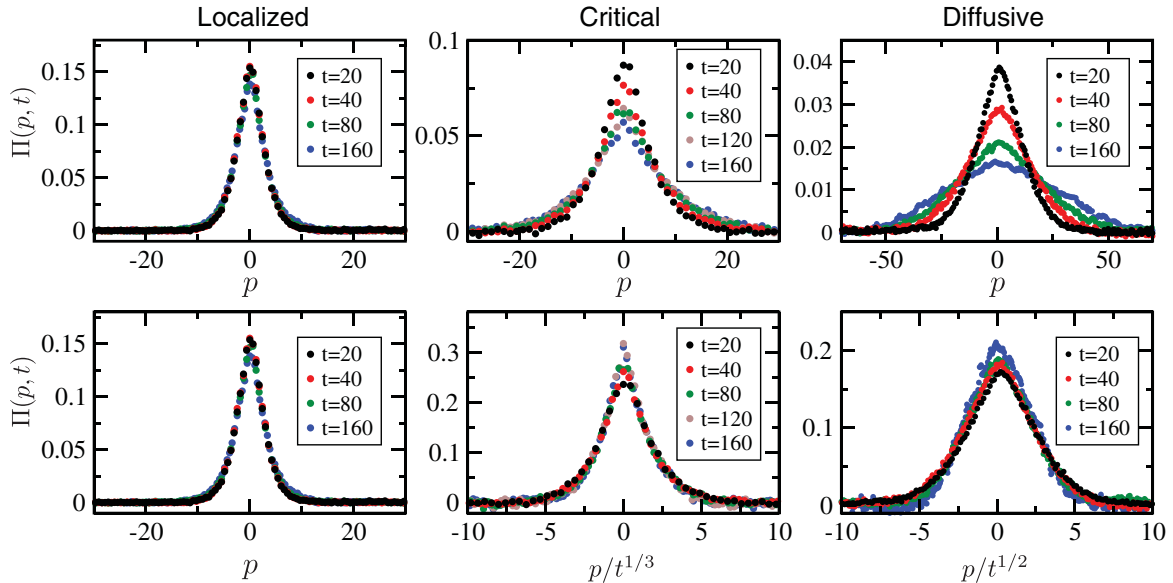


FIG. 1 (color). First row: Measured AIGF of the quasiperiodic atomic kicked rotor at different times $t$ in the (left to right) localized $(K, \varepsilon) = (4.5, 0.1)$, critical $(K = K_c, \varepsilon) = (6.3, 0.38)$ and diffusive $(K, \varepsilon) = (9.0, 0.8)$ regimes. Second row: Appropriate rescalings of the momentum by $t^0$ (localized), $t^{1/3}$ (critical), or $t^{1/2}$ (diffusive), bring the curves at different times into coincidence (the vertical scales are also rescaled in order to preserve normalization). The shapes are different in the three regimes: exponential localization, Eq. (1), in the localized regime, Gaussian shape, Eq. (2), in the diffusive regime, and the new "Airy shape," Eq. (6), at the critical point. Parameters are $\hbar = 2.89$, $\omega_2 = 2\pi\sqrt{7}$, $\omega_3 = 2\pi\sqrt{17}$. Time is measured in units of number of kicks and momentum in units of $2\hbar k_L$.

diffusive regimes. The three regimes obey different scaling laws. In the localized regime (left column), the momentum distribution is localized—i.e., it is time independent—at long times and thus scales as $t^0$. In the diffusive regime, the average kinetic energy $\langle p^2(t)\rangle$ increases linearly with time, so that the typical momentum scales as $t^{1/2}$; this is manifest in the broadening of the distribution with time seen in the right column. At the critical point of the Anderson transition, we observe [2,5], as predicted by the one parameter scaling theory [18,19], an anomalous diffusion $\langle p^2\rangle(t) \sim t^{2/3}$. This implies that the typical momentum scales as $t^{1/3}$ leading to a slower broadening of the distribution (middle column). If the raw experimental data are rescaled according to these laws (bottom row in Fig. 1), i.e., plotted vs $pt^0$, $pt^{-1/3}$, and $pt^{-1/2}$ in the localized, critical, and diffusive regimes, respectively, curves taken at various times coincide, which constitutes an experimental proof of the validity of the scaling laws (see [20] for a numerical study). The shapes of the distributions are different in the various regimes: exponential shape in the localized regime, Gaussian shape in the diffusive regime. The intermediate shape at the critical point is discussed below.

Figure 1 is a clear manifestation of the scaling properties. The anomalous diffusion is not a transient behavior and the AIGF keeps the same shape at the critical point. However, slightly off the critical point, the AIGF tends gradually to either a localized or diffusive behavior, following the anomalous diffusion only for short times. To confirm this observation over a time scale larger than 160 kicks, we performed numerical simulations of the critical dynamics up to $t = 10^6$ kicks. The result is shown in Fig. 2.
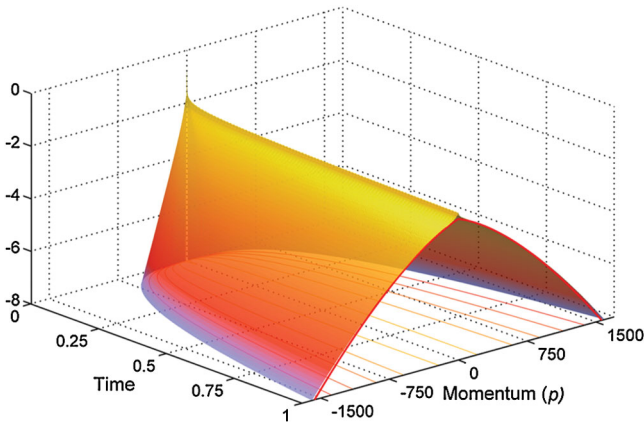


FIG. 2 (color). Numerically simulated time evolution of an initially localized momentum distribution (log scale), for the quasiperiodic kicked rotor at the critical point of the Anderson transition. The spreading follows an anomalous diffusion, with $\langle p^2(t)\rangle \propto t^{2/3}$, and the shape is identical at all times, being neither exponential (as it is in the localized regime), nor Gaussian (as it is in the diffusive regime). The analytic prediction, Eq. (6), is shown as the red thick curve at $1 \times 10^6$ kicks. The agreement is excellent, without any adjustable parameter. Parameters are those of Fig. 1. Time is measured in millions of kicks and momentum in units of two recoil momenta $2\hbar k_L$.

The advantage of numerical simulations is that it is possible to explore the tails of the momentum distributions (hidden by noise in a real experiment). The anomalous diffusion—with the characteristic subdiffusive $t^{1/3}$ scaling—is clearly visible. Obviously, the distribution is neither exponential (which would result in straight lines in the logarithmic plot), nor Gaussian (which would appear as a parabola in the logarithmic plot).

The form of the critical AIGF can be deduced from the self-consistent theory of localization [8]. This mean-field theory describes quantum transport in disordered systems at large distances and for long times (see, for example, [21]). It has been shown to be relevant for the 1D periodically kicked rotor [22] and correctly predicts a metal-insulator transition in three dimensions and the anomalous diffusion at the threshold: $D(\omega) \sim (-i\omega)^{1/3}$ with $\omega$ the frequency conjugated to time [23] (the 1/3 exponent is the counterpart in the frequency domain of the anomalous diffusion $\langle p^2\rangle(t) \sim t^{2/3}$ in the time domain).

Using this critical behavior, we can compute the AIGF for the quasiperiodic kicked rotor [24]. The details of the calculation will be published elsewhere; we obtain:

$$\Pi(p, t) = \tfrac{3}{2}(3\rho^{3/2}t)^{-1/3}\mathrm{Ai}[(3\rho^{3/2}t)^{-1/3}|p|], \qquad (6)$$

where $\rho$ is a parameter directly related to the critical quantity $\Lambda_c = \lim_{t\to\infty}\langle p^2\rangle/t^{2/3}$ (see [2,5]) via $\rho = \Gamma(2/3)\Lambda_c/3$, where $\Gamma$ is the Gamma function and $\mathrm{Ai}(x)$ is the Airy function. The asymptotic form Eq. (3) comes simply from the limiting behavior of the Airy function for large $x$ and is found perfectly intermediate between the exponential (localized) and the Gaussian (diffusive) shapes.

The analytic prediction, Eq. (6), matches very well the shape obtained from numerical simulations of the quasiperiodically kicked rotor shown in Fig. 2. The only noticeable difference is near $p = 0$, where the result of the numerical simulation is slightly larger than the analytic prediction. Note that this phenomenon, currently under study, is invisible on the time scale of the experiment (160 kicks).

Figure 3 shows the comparison between the experimentally measured critical AIGF and the analytic prediction, Eq. (6). The only fitting parameter is the global scale $\rho$; we find $\rho = 1.60$ for the best fit, which is in fair agreement with the theoretical prediction $\rho = \Gamma(2/3)\Lambda_c/3 = 2.04$. The difference can be attributed to several factors, the most important ones (roughly 10% each) being finite-time effects and residual decoherence which both tend to shift the effective critical point to lower $\Lambda$, i.e., lower $\rho$.

Although it is visually not obvious to distinguish the observed shape from either an exponential shape or a Gaussian shape, a careful fitting procedure gives a clear cut result. The residual between the observed distribution and the analytic prediction (6), shown in panel (b), is consistently zero (within the error bars), while a fit with
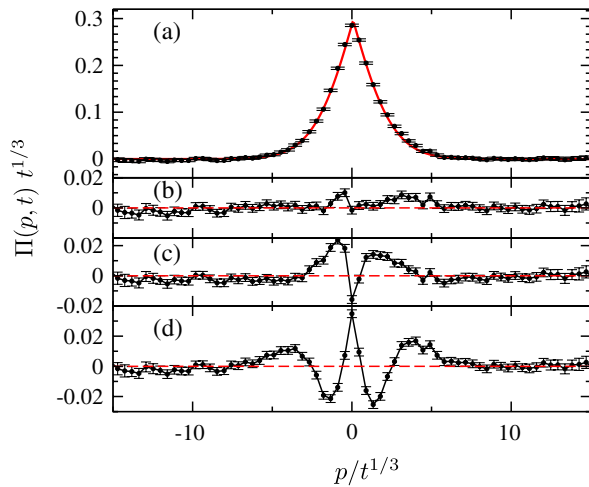
FIG. 3 (color online).   (a) Experimental data for the rescaled critical AIGF (see Fig. 1) averaged over time (black circles with error bars) and a fit given by Eq. (6), with $\rho$ as the only fitting parameter. The agreement is clearly excellent. The residual does not significantly differ from zero [panel (b)]. Fits by an exponentially localized (c) or a Gaussian (d) distribution show significant deviations.

an exponential shape, panel (c), or a Gaussian shape, panel (d), displays significant deviations. This is fully confirmed by a quantitative check of the quality of the fit. The fit by the Airy function gives a $\chi^2$ per degree of freedom equal to 1.09—i.e., perfectly acceptable—while the exponential fit gives 4.5 per degree of freedom and the Gaussian fit 8.8, two unacceptably large values. This clearly shows that the self-consistent theory of localization accounts for the critical AIGF and its scaling properties.

In conclusion, we have studied experimentally the transport at the threshold of the Anderson transition. It obeys (temporal) scale invariance, a fundamental property of second-order phase transitions, and this defines a new state, between an insulator and a metal. Its analytic form can be deduced from the self-consistent theory of localization. Work is in progress to allow experimental observations at longer times, which should allow us to characterize the small deviations observed numerically, whose origin could be multifractality.

*Present address: Service de Physique de l'Etat Condensé (CNRS URA 2464), IRAMIS/SPEC, CEA Saclay, F-91191 Gif-sur-Yvette, France
†Present address: Laboratoire Aimé Cotton, Université Paris-Sud, Bâtiment 505, Campus d'Orsay, F-91405 Orsay Cedex, France
‡www.phlam.univ-lille1.fr/atfr/cq

[1] J. Cardy, *Scaling and Renormalization in Statistical Physics* (Cambridge University Press, Cambridge, 1996).
[2] J. Chabé *et al.*, Phys. Rev. Lett. **101**, 255702 (2008).
[3] P. W. Anderson, Phys. Rev. **109**, 1492 (1958).
[4] F. Wegner, Z. Phys. B **25**, 327 (1976).
[5] G. Lemarié *et al.*, Phys. Rev. A **80**, 043626 (2009).
[6] G. Lemarié, B. Grémaud, and D. Delande, Europhys. Lett. **87**, 37007 (2009).
[7] K. Slevin and T. Ohtsuki, Phys. Rev. Lett. **82**, 382 (1999); A. Rodriguez *et al.*, Phys. Rev. Lett. **105**, 046403 (2010).
[8] D. Vollhardt and P. Wölfle, in *Electronic Phase Transitions*, edited by W. Hanke and Y. V. Kopaev (Elsevier, Amsterdam, 1992), pp. 1–78.
[9] S. Faez *et al.*, Phys. Rev. Lett. **103**, 155703 (2009).
[10] F. L. Moore *et al.*, Phys. Rev. Lett. **75**, 4598 (1995).
[11] J. Billy *et al.*, Nature (London) **453**, 891 (2008).
[12] R. Kuhn *et al.*, New J. Phys. **9**, 161 (2007).
[13] S. Aubry and A. André, Ann. Isr. Phys. Soc. **3**, 133 (1980); G. Roati *et al.*, Nature (London) **453**, 895 (2008); M. Albert and P. Leboeuf, Phys. Rev. A **81**, 013614 (2010).
[14] G. Casati, I. Guarneri, and D. L. Shepelyansky, Phys. Rev. Lett. **62**, 345 (1989).
[15] D. M. Basko, M. A. Skvortsov, and V. E. Kravtsov, Phys. Rev. Lett. **90**, 096801 (2003).
[16] J. Ringot, Y. Lecoq, J. C. Garreau, and P. Szriftgiser, Eur. Phys. J. D **7**, 285 (1999).
[17] J. Ringot, P. Szriftgiser, and J. C. Garreau, Phys. Rev. A **65**, 013403 (2001).
[18] E. Abrahams, P. W. Anderson, D. C. Licciardello, and T. V. Ramakrishnan, Phys. Rev. Lett. **42**, 673 (1979).
[19] T. Ohtsuki and T. Kawarabayashi, J. Phys. Soc. Jpn. **66**, 314 (1997).
[20] F. Borgonovi and D. Shepelyansky, Physica D (Amsterdam) **109**, 24 (1997).
[21] H. Hu *et al.*, Nature Phys. **4**, 945 (2008).
[22] A. Altland, Phys. Rev. Lett. **71**, 69 (1993).
[23] B. Shapiro, Phys. Rev. B **25**, 4266 (1982).
[24] G. Lemarié, Ph.D. thesis, Université P. et M. Curie, Paris, 2009.